Iranian Polymer Journal (2021) 30:135–147
https://doi.org/10.1007/s13726-020-00879-5

ORIGINAL RESEARCH

Thermal behavior and water absorption kinetics of polylactic acid/chitosan biocomposites

Nor Helya Iman Kamaludin[1,2] · Hanafi Ismail[1] · Arjulizan Rusli[1] · Sam Sung Ting[2,3]

Received: 9 April 2020 / Accepted: 9 October 2020 / Published online: 26 October 2020

Abstract

In this study, biodegradable polylactic acid (PLA)/chitosan (Cs) composites were produced via melt compounding and compression molding techniques. Various chitosan loadings of 2.5, 5, 7.5 and 10 parts per hundred parts of polymer (php) were incorporated into PLA and its effects on thermal, water absorption kinetics, tensile and morphological characteristics were investigated systematically. Thermal analysis indicated that an increase in chitosan loading of up to 10 php enhanced the crystallinity percentage (χ_c) of neat PLA to an extent of 51%, yet reduced the thermal stability of the resulting biocomposites. The kinetic study results revealed that water absorption of PLA/Cs biocomposites approached the Fickian diffusion behavior. The maximum water uptake (M_{sat}) increased with chitosan addition, which can be attributed to stronger water–filler interaction. This was correlated to higher diffusion (D), solubility (S) and permeability (P) coefficients, which suggested the acceleration in diffusion rate and better water permeation through the biocomposites. In addition, the tensile results of dry samples showed enhancement in tensile strength and tensile modulus by 2% and 14%, respectively, relative to neat PLA through the incorporation of 2.5 php of chitosan loading. However, the water-immersed biocomposites demonstrated deterioration in all tensile properties (tensile strength, tensile modulus, and elongation-at-break values) which signified hydrolytic polymer degradation. This was confirmed by the FESEM micrographs of the fractured surfaces which exhibited filler pulled-out phenomenon and cavity formation after 50 days of water immersion.

Keywords Polylactic acid · Chitosan · Biocomposite · Thermal behavior · Water absorption kinetics

Introduction

Issues on environmental problems associated with plastic waste are most often being highlighted. In 2010, Malaysia was ranked as one of the world's worst plastic-polluted countries which generated about 0.94 million tons (MT) of mismanaged plastic wastes (wastes that are inefficiently disposed or recycled). The volume of plastic wastes going into the ocean is set to quadruple until 2050 [1]. Moreover, carbon emissions associated with plastic, starting from its production to burning, had reached 860 MT in 2019, which was greater than the annual emissions of Thailand, Vietnam, and the Philippines [2]. Therefore, due to the environmental concern and governance legislation, academic and industrial researchers are proactive in discovering a new alternative by producing biodegradable and eco-friendly composite materials which are sometimes known as biocomposites [3]. These green materials serve as substitute for synthetic polymers derived from petrochemical based-products which are non-renewable and non-biodegradable [4].

Therefore, polylactic acid (PLA) is interestingly applied as a polymer matrix due to its processability, renewability, biodegradability and biocompatibility properties [5, 6]. Moreover, it imparts comparable mechanical properties notably tensile modulus to commodity polymers of polypropylene, polyethylene, and polystyrene [7, 8], which provide attractive alternatives, particularly in food packaging products. PLA consists of linear aliphatic thermoplastic polyester which is generally synthesized either by direct

✉ Hanafi Ismail
ihanafi@usm.my

[1] School of Materials and Mineral Resources Engineering, Engineering Campus, Universiti Sains Malaysia, 14300 Nibong Tebal, Pulau Pinang, Malaysia

[2] Faculty of Chemical Engineering Technology, Universiti Malaysia Perlis, 02600 Arau, Perlis, Malaysia

[3] Center of Excellence Geopolymer and Green Technology (CEGeoGTech), Universiti Malaysia Perlis, 01000 Kangar, Perlis, Malaysia

poly-condensation or ring-opening polymerization of lactic acid monomers. The lactic acid monomer is derived by means of bacterial fermentation of agricultural products (corn, sugar cane, and potato) [9, 10]. However, due to its high manufacturing cost (US$ 3.80/kg) [11], poor gas barrier properties [12] and relatively low thermomechanical stability [13], PLA usage is restricted for wider applications. Therefore, the incorporation of PLA with natural fillers could be a favorable strategy to minimize these inherent properties. Apart from environmental and economic concerns [14], the addition of natural fillers could improve product properties and performance [15].

Several studies have investigated the incorporation of natural fillers into PLA, which are mainly derived from polysaccharides derivatives of agro-polymers, including starch (cassava, corn, and sago starch) [16–18], cellulose (coir fiber and wood fiber) [8, 19], chitin, and chitosan [20]. Nonetheless, in this study chitosan was preferred based on its unique properties.

Chitosan is a cationic polysaccharide produced from alkaline the deacetylation reaction of chitin extracted from the cell walls of fungi, exoskeleton of crustaceans and arthropods [21]. Chitosan is abundantly available, biodegradable [22], and non-toxic, which is recognized as safe (GRAS) category, and thus makes it suitable for countless applications, especially in food packaging (food wrappings and containers, drinking bottles) and biomedical field (drug delivery or medical devices) [12]. Now, various preparation methods, such as solution casting, extrusion, electrospinning, and melt compounding are applied to prepare composite films or mats.

However, variation in processing and environmental exposure could affect the properties of the resulting biocomposite. Râpă et al. [20] revealed that the degree of crystallinity of the plasticized PLA/Cs system was enhanced by 18%, but a significant decrease was observed in tensile strength and Young's modulus relative to the neat PLA. Moreover, PLA/Cs film prepared by solution casting technique showed a reduction in the decomposition temperature and thermal stability with increasing chitosan content [5].

Another study performed by Bonilla et al. [13] found that the chitosan did not influence thermal behavior and degree of crystallinity of PLA/Cs films prepared by extrusion, but it increased the film extensibility. In addition, due to hydrophilicity of chitosan, the exposure of biocomposite to humid environment could diminish the tensile properties and affect the degradability of materials. Correlo et al. [23] reported that the PLA/Cs blend showed a significant reduction in ultimate tensile strength and maximum hydrolytic degradation due to the higher water uptake that could weaken the interfacial bonds between a natural filler and relatively polymer matrices, which consequently affected the product shelf life [24, 25].

Therefore, the water penetration mechanism through the composite materials has induced a new water absorption pathway that must be understood. Leu and Chow [7] reported on water absorption kinetics of PLA/organomontmorillonite (OMMT)/poly(ethylene glycol) (PEG) nanocomposites. The report revealed that the diffusivity was reduced by 50% with the incorporation of OMMT and 3 phr of PEG. This remarkable reduction was attributed to the plasticization effect of PEG which enhanced the tortuous path and water-barrier properties of PLA.

In another study by Chung et al. [26], the water absorption resistance of the acetylated kenaf-PLA composites was observed. The study reported that the composite with treated fibers exhibited a low water uptake rate due to a reduction in composite water affinity as a result of the replacement of the hydroxyl sorption sites by acetyl groups. Besides, Aranda-Garcia et al. [27] mentioned that the reduction in moisture absorption rate with agave bagasse fiber incorporated into thermoplastic starch/PLA blends was due to the low fiber hydrophilicity. Furthermore, Móczó et al. [28] revealed an increase in water absorption capacity with an increase in starch content of PLA composites.

Therefore, the study on thermal behavior and water absorption kinetics of natural filler incorporated into biopolymer at various loadings is essential in controlling the convenience rate of water diffusion and determining its thermal and hydrolytic degradations. This is important to adequately tackle its efficient usage in a wide range of applications and attain its desired performance. To the best of our knowledge, no research was performed to investigate the water absorption kinetics of PLA/Cs biocomposites. However, limited work was reported on the thermal properties of the resulting biocomposites at varying chitosan loadings [5, 20].

Therefore, this current study aims to investigate the effect of chitosan loadings on thermal behavior, water absorption kinetics, tensile and morphological characteristics of PLA/chitosan biocomposites prepared via melt compounding technique that is industrially oriented.

Experimental

Materials

The polylactic acid (PLA) pellets of 4032D type used in this study were supplied by NatureWorks LLC (USA) and had a specific gravity of 1.24 and melt mass flow rate (MFR) of 7 g/10 min at 210 °C/2.16 kg. Chitosan (Cs) powder with a degree of deacetylation of 90.5%, a molecular weight of 700 kDa, a viscosity of 62 cP and particle size in the range of 10–80 μm was purchased from Cleo International Trading (Shanghai) and used as the filler.

Preparation of PLA/Cs biocomposites

Melt compounding of PLA at different chitosan loadings was conducted using an internal mixer (Thermo Haake Polydrive, Model R600/610, Germany) operated at a processing temperature of 180 °C and 60 rpm of rotor speed for 10 min. Two sets of specimens were prepared in dry (prior immersion) and wet (after immersion) conditions. The samples' composition of chitosan was 0, 2.5, 5, 7.5, and 10 parts per hundred parts of polymer (php), which were designated as neat PLA, PLA/2.5Cs, PLA/5Cs, PLA/7.5Cs, and PLA/10Cs, respectively.

Due to their hygroscopic nature, both PLA pellets and chitosan powders were pre-dried overnight in a vacuum oven at 60 °C and 105 °C, respectively, to remove moisture prior to use. Once the melted samples were obtained, the dumbbell sheet (ASTM D638) of PLA/Cs biocomposites were fabricated using a compression molding machine (GoTech, RT-7014A, Taiwan) with a hydraulic press pressure of 7 MPa at 180 °C for 3 min. The same condition was applied for the preparation of the neat PLA sample, which was used as a reference.

Thermal analysis

DSC

The thermal behavior study of PLA-based biocomposite was conducted using a differential scanning calorimeter (DSC) (Perkin Elmer, Pyris 6, USA), in accordance with Dong et al. [29] but with a slight modification. Approximately 10 mg of sample was capsulated on aluminum pans prior to heating and cooling cycles. The measurement was performed in two heating cycles at a scan rate of 10 °C/min under nitrogen gas flow with a temperature from 30 to 190 °C.

After the first heating cycle was completed, the isothermal condition remained for 5 min at 190 °C to eliminate the thermal history. Next, the sample was cooled at 10 °C/min from 190 to 30 °C, followed by a second heating step at the same heating rate. The thermal variables of glass transition temperature (T_g), cold crystallization temperature (T_{cc}), melting temperature (T_m), cold crystallization enthalpy (ΔH_{cc}) and fusion enthalpy (ΔH_m) were identified by the respective peak and area under a curve. Moreover, the percentage of crystallinity (χ_c) was evaluated by the following equation [29]:

$$\chi_c = \left[\frac{\Delta H_m - \Delta H_{cc}}{\left(\Delta H_m^\circ \times W_{PLA}\right)}\right] \times 100\%, \quad (1)$$

where χ_c is the degree of crystallinity, ΔH_m and ΔH_{cc} are the enthalpy of fusion and enthalpy of cold crystallization of PLA in the biocomposites, respectively. ΔH_m° is the enthalpy of fusion of 100% crystalline PLA (93.6 J/g) [7] and W_{PLA} is the mass fraction of PLA in the biocomposites.

TGA

The thermal stability and decomposition of PLA-based biocomposites were investigated using a thermogravimetric analyzer (TGA) (Perkin Elmer, Pyris 6, USA), as described by Tham et al. [30]. Approximately 10 mg of sample was applied and the test was performed under a nitrogen atmosphere (50 mL/min) at a scanned temperature range of 30 to 600 °C with a heating rate of 10 °C/min. Then the thermal weight loss at its derivative temperature was recorded.

Water absorption analysis

The investigation on water absorption of PLA/Cs biocomposites was performed in accordance with ASTM D570. The process was done by fully immersing the specimens in distilled water (pH 6.6) under ambient temperature and at different time intervals until saturation was attained. Initially, the prepared dumbbell specimens were oven-dried at 60 °C until a constant weight (m_i) was reached. After 24 h of immersion, specimens were removed from the water, instantly wiped off with a dry tissue, and subsequently weighed (m_t) using an analytical balance. The process was repeated over 50 days of water immersion. The percentage of water uptake (WU) was determined according to Petchwattana et al. [31], as shown in the following equation:

$$\mathrm{WU}(\%) = \frac{m_t - m_i}{m_i} \times 100, \quad (2)$$

where m_i and m_t denote the mass of oven-dried and mass at time t after water immersion, respectively.

Tensile property analysis

The investigation on tensile properties of dry and wet (immersed) specimens was determined according to ASTM D638. The tensile analysis was conducted using the universal testing machine (Instron, Model 3366, USA), which was operated under 1 kN of load cell and 5 mm/min of crosshead speed. Five dumbbell specimens with 1 mm thickness were tested for each composition (i.e., 0, 2.5, 5, 7.5, and 10 php of Cs loading) and conditions (dry and wet). The stress–strain curve was observed and the average values of tensile strength, tensile modulus, and elongation-at-break of each composition were reported.

Morphological analysis

The morphology characteristics of a tensile fracture surface of pure PLA and PLA/Cs biocomposites of both specimens (dry and wet) were investigated using a field emission scanning microscope (FESEM) (Zeiss, Supra 35 VP, Germany). The specimens were mounted onto aluminum stubs and sputter-coated with a gold thin layer and were observed under 10 kV accelerating voltage. The tensile fracture surface morphological characteristics specimens were examined at 300 × magnification.

Results and discussion

DSC analysis of PLA/Cs biocomposites

Figure 1 demonstrates the differential scanning calorimetry (DSC) thermograms of pure chitosan, neat PLA and PLA/Cs biocomposites, which were recorded from the second heating cycle at a heating rate of 10 °C/min. Through the DSC curves, the related thermal phase transition properties of glass transition temperature (T_g), cold crystallization temperature (T_{cc}), melting temperature (T_m), cold crystallization enthalpy (ΔH_{cc}), fusion enthalpy (ΔH_m) and percentage of crystallinity (χ_c) were assessed and are tabulated in Table 1.

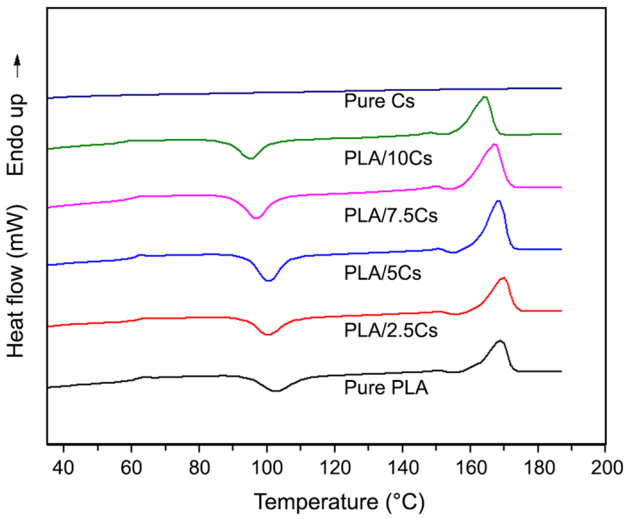

Fig. 1 DSC thermograms of the second heating cycle of pure chitosan, pure PLA, and PLA/Cs biocomposites at various chitosan loadings

As presented in Fig. 1, neat PLA and PLA/Cs biocomposites showed slight deviations in various phase transition temperatures with the increase in chitosan loading. For pure chitosan, no obvious peak was observed as the specimens were heated from ambient temperature to 190 °C. This was attributed to the non-appearance of crystalline nature in pure chitosan samples, as reported by Han et al. [5]. Meanwhile, the T_g of PLA/10Cs biocomposite decreased by 5 °C in comparison with pure PLA. The reduction in the T_g suggested that the presence of short chitosan chains generated more free volume which facilitated PLA chain mobility, and thus allowed the reorganization of the amorphous domain. Besides, longer melt processing of 10 min could also promote the thermal degradation of neat PLA and its biocomposites as the samples completely melted and reached stabilization torque after 7 min of mixing time. This is associated with the reduction of heat capacity, $C_{p,}$ from 1.79 to 0.26 J/g.°C with increasing filler loading indicating less entanglement of PLA polymer chains leads to a reduction in T_g. The result was in line with the studies reported by Pal and Katiyar [32] and Li and Huneault [33] which suggested that the processing conditions could affect PLA polymer degradation.

Furthermore, the T_{cc} decreased from 100.6 to 95.2 °C by filler addition, as opposed to 102.6 °C of neat PLA. This can be explained that upon heating, the crystallization of PLA occurred at a lower temperature in the system with greater flexibility and higher molecular chain mobility. This allowed easier chain segments movement into the crystallization sites, and thus enhanced the crystallization ability and crystalline degree [34].

Neat PLA represents a relatively low crystallinity (χ_c) degree of 13.6%, implying that it is poorly crystallized. However, an enhancement of up to 51% degree of crystallinity was noticed with added chitosan of 10 php. The

Table 1 Thermal characteristic of the second heating cycle of pure Cs, neat PLA, and PLA/Cs biocomposites at various chitosan loadings

Sample code	T_g (°C)	T_{cc} (°C)	ΔH_{cc} (J/g)	T_m (°C)	ΔH_m (J/g)	χ_c (%)
Pure Cs	–	–	–	–	–	–
Neat PLA	62.5	102.6	20.5	169.0	33.2	13.6
PLA/2.5Cs	61.1	100.6	22.2	169.5	36.9	16.1
PLA/5Cs	60.0	100.3	24.7	168.3	41.5	18.9
PLA/7.5Cs	58.5	96.7	25.1	167.3	42.1	19.5
PLA/10Cs	57.7	95.2	27.8	164.8	45.6	20.6

The values of T_g, T_c, T_m, ΔH_{cc}, and ΔH_m were obtained from peak and area under the DSC thermatograms from Pyris software and Eq. (1) was used for the calculation of crystallinity percentage

results suggested that chitosan might perform as a nucleating agent in PLA/Cs biocomposites, whereby crystallization was induced at a lower temperature. This was in agreement with the results reported by Tee et al. [35] which indicated the capability of hydrophilic cellulose to act as an effective nucleating agent in PLA because it promoted crystallization at lower temperatures.

In addition, the neat PLA and its biocomposites exhibited a unimodal single endothermic melting peak in the range of 164.8–169.5 °C, which proposed the existence of α-crystalline form and homogeneous crystal distribution [32]. Nonetheless, the melting temperature (T_m) of pristine PLA had shifted to the lower value with an increase in chitosan content. This may be associated with the instability of PLA crystals due to the chitosan agglomeration with higher filler addition. Greater thermal energy (ΔH_m) supports higher crystallinity of PLA/Cs biocomposites as it increased with Cs loading indicating more energy is needed to break the crystalline structure in order to allow the changing of polymer into a molten state.

TG and DTG analyses of PLA/Cs biocomposites

The thermal stability and decomposition of PLA-based biocomposites were analyzed under thermal gravimetric analysis. TGA and DTG curves of PLA/Cs biocomposites at various chitosan contents are illustrated in Fig. 2a, b, respectively. For pure chitosan, three significant stages of weight loss were identified. The first stage was observed at a temperature range of 40–130 °C, which was ascribed by the moisture vaporization resulted from the disappearance of adsorbed water by the hydrophilic chitosan. The second stage begins at 250 °C and indicated the maximum weight loss rate at 300 °C. Meanwhile, the third stage was overlapping with the end of the second stage that exhibited the maximum weight loss rate at 370 °C, which then proceeded above 600 °C. The total weight loss of both stages was ~ 52%. This could be due to the breakdown of the saccharide structure in chitosan molecules, including saccharide rings and chitin products of acetylated and deacetylated units by dehydration and decomposition reactions, as suggested by Han et al. [5].

For pure PLA, a single weight-loss stage was inspected in the range of 300–390 °C with the maximum rate at 360 °C and total weight loss of ~ 98%. This was ascribed by the degradation of the ester bonds including cyclic oligomers, lactide and acetaldehyde molecules, as well as, carbon monoxide gaseous release [21, 36].

Similar trends were presented by PLA/Cs biocomposites as their decomposition occurred in a single-step process and the main thermal peak occurred at 260–380 °C, which represented weight loss in the range of ~ 93–98% with chitosan addition of 2.5 php to 10 php. This indicated that the decomposition of the PLA polymer and chitosan components occurred simultaneously in the biocomposites. Besides, PLA-based biocomposites promoted better thermal stability as compared to pure chitosan because higher decomposition temperature (T_{max}) of above 310 °C was observed for them. However, neat PLA exhibited higher thermal stability than its biocomposites. This was attributed to the low degradation temperature and poor thermal stability of chitosan. The results were consistent with Rodríguez-Núñez et al. results [37] which observed decreasing in thermal stability and decomposition

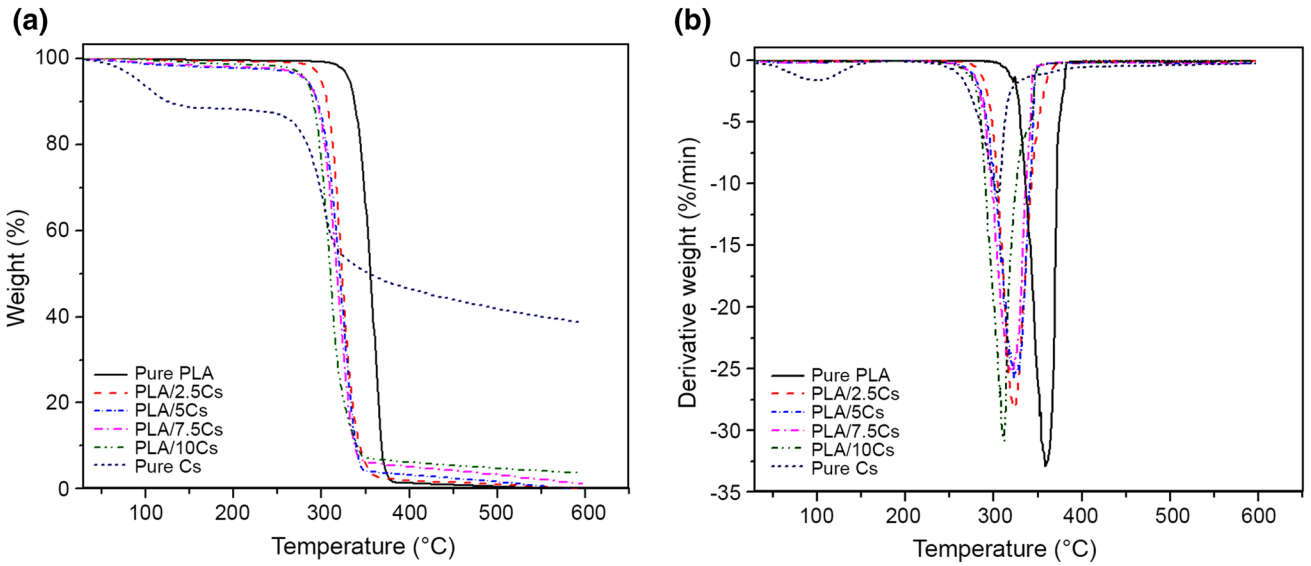

Fig. 2 **a** TGA and **b** DTG curve of pure chitosan, pure PLA and PLA/Cs biocomposites at 2.5, 5, 7.5, and 10 php of chitosan loadings

Table 2 TG and DTG data of pure Cs, neat PLA, and PLA/Cs biocomposites at various chitosan loadings

Sample code	TG			DTG	
	$T_{10\%}$ (°C)	$T_{50\%}$ (°C)	$T_{90\%}$ (°C)	T_{max} (°C)	Weight loss at T_{max} (%)
Pure Cs	126	354	–	305	36.1
Neat PLA	337	355	368	359	61.1
PLA/2.5Cs	306	324	344	326	57.8
PLA/5Cs	295	321	340	324	57.7
PLA/7.5Cs	294	318	339	320	55.4
PLA/10Cs	290	310	338	312	55.0

The values of $T_{0.1}$, $T_{0.5}$, $T_{0.9}$, T_{max} and percentages of weight loss were obtained from TGA thermatograms as shown in Fig. 2

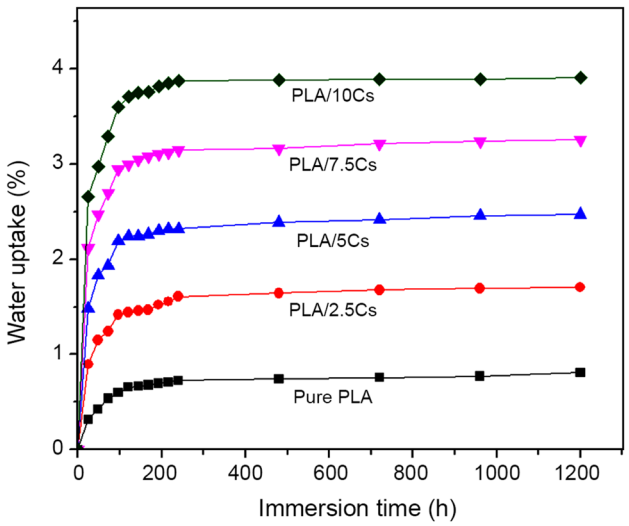

Fig. 3 Water uptake characteristics of PLA and PLA/Cs biocomposites for various chitosan loadings against immersion time

temperature as chitosan and/or thermoplastic starch (TPS) were incorporated into the PLA matrix.

Table 2 summarizes the thermal stability variables of $T_{10\%}$, $T_{50\%}$, $T_{90\%}$ and T_{max} which represent the degradation temperature that occurred by 10%, 50%, 90% of weight loss and the maximum decomposition temperature, respectively. It was demonstrated that the thermal decomposition temperature decreased with chitosan addition.

A similar trend was reported by Zaaba and Ismail [17] in their study on the thermogravimetric stability of PLA/thermoplastic corn starch (TPCS) biocomposites. This was ascribed to lower thermal stability at higher chitosan content as a result of the reduction of interfacial interaction between the chitosan filler and PLA matrix. This facilitated the autocatalytic cleavage of carbon–carbon bonds during the chain scission process; hence, lowered the decomposition temperature [5].

Increasing the filler loading to 10 php contributed to the decrease in weight loss at T_{max} by 2.8%, which further clarified the occurrence of the maximum polymer degradation at a single stage. This was in agreement with the results observed by Pal and Katiyar [32] in the preparation of PLA with functionalized chitosan. Also, the maximum weight loss rate of PLA/Cs biocomposites occurred at lower temperatures (312–326 °C) than that of the neat PLA (359 °C) signified that chitosan addition accelerated the decomposition reaction of the biocomposites.

Water absorption characteristics and kinetics

The characteristics of water uptake by PLA/Cs biocomposites at varying chitosan contents are displayed in Fig. 3. At the initial stage, the neat PLA exhibited a slow rate of water absorption with the first plateau attained at around 96 h, and the maximum water uptake was only 0.81%. This can be explained by the hydrophobicity of the PLA polymer matrix as stated by Correlo et al. [23], which tends to absorb less water, and thus promoted the lowest water absorption.

Contrary to the PLA-based biocomposites, the water absorption increased drastically at the beginning of the process until 120 h of water immersion, followed by a slow absorption rate until it reached equilibrium. Moreover, the maximum percentage of water uptake increased from 1.71 to 3.91% with the incorporation of chitosan filler of 2.5 php and 10 php, respectively. This was attributed to the hydrophilicity of chitosan which enhanced water-filler interaction. At higher chitosan content, more free hydroxyl groups were present in the chitosan, and thus induced higher interaction with water molecules through hydrogen bonding formation, as illustrated in Scheme 1. This significantly results in weight increment and a rise in water absorption. The finding was in agreement with Zubir et al. [38] who observed greater water uptake with increased rice straw particulate content in the polylactic acid/polyhydroxybutyrate–valerate blends. Yet, the biocomposite with lower chitosan content reached saturation more rapidly, which suggested a limited water–filler interaction.

In addition, apart from filler agglomeration, poor impregnation during processing could affect the biocomposite system [39]. This contributes to the generation of micro-gaps and micro-cracks at the matrix–filler interface (as shown later in the morphology study), and thus promotes the diffusion of water molecules through the generated microstructure within the polymer matrix. However, the water absorption of this biocomposite was considered to be lower ($M_{sat} < 5.0\%$) as compared to the modified chitosan film which exhibited greater water uptake of up to 10%, as reported by Cui et al. [40] in their study finding. This indicated the capabilities of these newly prepared biocomposites

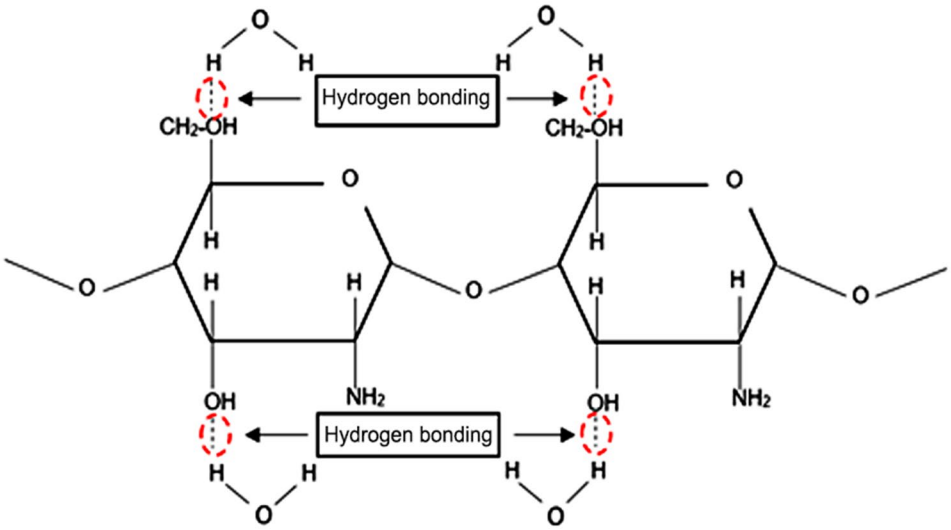

Scheme 1 Proposed interaction between water molecules and chitosan during water absorption process in PLA/Cs biocomposites

to adapt to the humid environment for their wide potential applications.

A similar trend of water absorption characteristics was exhibited in all biocomposites formulations which demonstrated single steps of absorption. The water absorption process started with a linear and sharp increase at the beginning, then proceeded at slower rates and finally approached the saturation stages after an extended immersion time of 1200 h. A similar finding was reported by Lukitowati and Indrani [41] who studied the water absorption of chitosan membranes with gamma-ray irradiations. This water absorption behavior can be modeled as a Fickian type diffusion process, as reported by Leu and Chow [7] and Muñoz and García-Manrique [39] in their studies.

The investigation on water absorption was extended by analyzing the diffusion mechanism and kinetics of PLA/Cs biocomposites according to Fick's law theory. Generally, three known mechanisms were involved in the water diffusion of polymer composites, including Fickian, relaxation controlled and anomalous or non-Fickian diffusion [42]. To analyze the water absorption kinetics, the experimental data were fitted into the sorption curves, as demonstrated by the relation stated by Petchwattana et al. [31] as follows:

$$\frac{M_t}{M_{sat}} = kt^n. \tag{3}$$

By writing Eq. (3) in the log form,

$$\log \frac{M_t}{M_{sat}} = \log(k) + n\log(t), \tag{4}$$

where M_t and M_{sat}, respectively, represent the water uptake at immersion time t and saturation point. The constants k and n are estimated from the intercept and slope of the log plot of $\left(\frac{M_t}{M_{sat}}\right)$ against time, respectively. The absorption mechanism is attributed by the n value; for Fickian diffusion, $n = 0.5$; for relaxation control, $n \geq 1.0$; and for the non-Fickian (anomalous), $0.5 < n < 1.0$, as indicated by Adhikary et al. [43].

Figure 4 illustrates the experimental data fitting of PLA-based biocomposites at various chitosan loadings. The k and n values are directly estimated from the linear regression analysis in between log(t) of 1.4 and 2, as listed in Table 3. The log(t) values of above 2 were not considered due to slower water absorption and approach to saturation. It was found that all biocomposites formulations showed n values of less than 0.5 ($n < 0.5$). This was acceptable and the results suggested that the water absorption of PLA/Cs biocomposites approached the Fick's model as the n value in the range of 0.12–0.43 is considered as a Fickian diffusion,

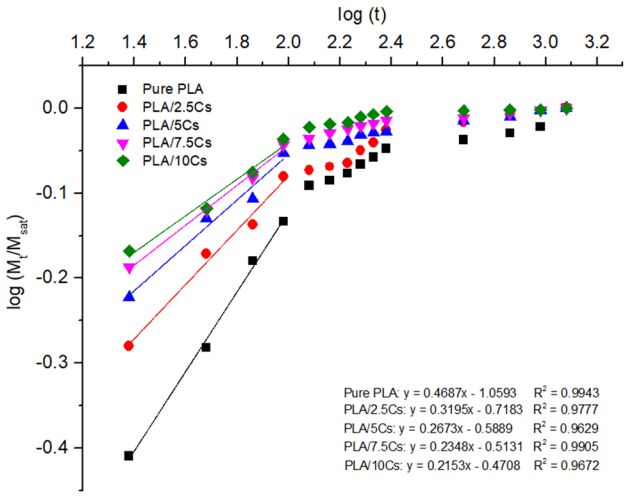

Fig. 4 Plots of $\log\left(\frac{M_t}{M_{sat}}\right)$ versus $\log(t)$ of PLA and PLA/Cs biocomposites for various chitosan loadings

Table 3 Kinetics constants of PLA and PLA/Cs biocomposites

Sample code	*n*	*k*
PLA	0.4687	0.0872
PLA/2.5CS	0.3195	0.1913
PLA/5CS	0.2673	0.2577
PLA/7.5CS	0.2348	0.3068
PLA/10CS	0.2153	0.3382

The values of n and k were obtained from the slope and y-intercept of $\log \frac{M_t}{M_{sat}}$ versus $\log(t)$ plot by applying Eq. (4)

as reported by Witono et al. [44] in their study on water absorption characteristics of cassava starch grafted with polyacrylic acid.

Furthermore, the k value which increased with increasing filler loading indicated that a shorter time was needed for the biocomposite to attain saturation and confirmed the water absorption increment. Besides, the R^2 values of all formulations were close to one, which implied that experimental data fitted well to the studied model.

Next, the rate of water transport was analyzed by determining the values of diffusion coefficient, D. This was examined as an essential variable in Fick's model in explaining the water molecules' capability to permeate through the polymeric composites. Since water absorption followed the Fickian diffusion pattern, it can be explained using the relation stated by Muñoz and García-Manrique [39] as follows:

$$\frac{M_t}{M_{sat}} = 4\sqrt{\frac{Dt}{\pi L^2}}, \tag{5}$$

where L indicates the specimen thickness.

At early absorption stages, water absorption at time t (M_t) increased linearly with $\sqrt{t}$. Therefore, by rearranging Eq. (5), the average water diffusion coefficient (D) can be determined through the absorption curve pattern represented by the following equation:

$$\frac{M_t}{M_{sat}} = \frac{4}{L}\left(\frac{D}{\pi}\right)^{0.5} t^{0.5}. \tag{6}$$

The water diffusion coefficient (D) of PLA/Cs biocomposites is presented in Table 4 as it was estimated from the initial slope of $\left(\frac{M_t}{M_{sat}}\right)$ against $(t)^{0.5}$ plot, which is illustrated in Fig. 5. It was observed that at the early stage, water absorption increased gradually with $(t)^{0.5}$; subsequently, tended to flatten out to the saturation point with prolonged immersion time. Moreover, the diffusion coefficient, D, was directly proportional to the filler loading as it is raised with increased chitosan loading. This could be elucidated by the chitosan agglomeration at higher filler loading, and thus promoted micro-crack generations at the filler-matrix interface (as shown in the morphology study). This induced chitosan dissolution due to the swelling effect; hence, accelerated the water transport, leading to a higher diffusion rate. This characteristic was in agreement with Petchwattana et al. [31] which observed that higher hydrophilic wood flour content would promote greater water

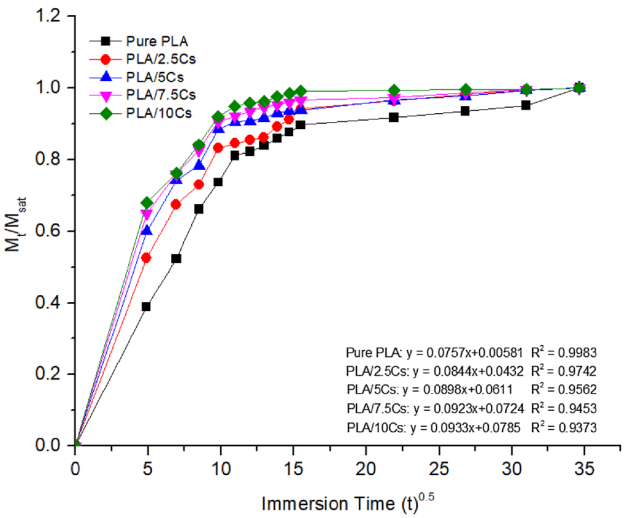

Fig. 5 Plots of $\frac{M_t}{M_{sat}}$ versus $t^{0.5}$ of PLA and PLA/Cs biocomposites for various chitosan loadings

Table 4 Maximum water absorption, diffusion coefficient, solubility, and permeability variables of PLA and PLA/Cs biocomposites

Sample code	Maximum water absorption M_{sat} (%)	Diffusion coefficient $D\times10^{-13}$ (m^2/s)	Solubility S (g/g)	Permeability $P\times10^{-14}$ (m^2/s)
Pure PLA	0.809	3.1111	0.0081	0.2520
PLA/2.5CS	1.705	3.8889	0.0170	0.6611
PLA/5CS	2.472	4.4167	0.0247	1.0909
PLA/7.5CS	3.255	4.6389	0.0326	1.5123
PLA/10CS	3.910	4.7500	0.0391	1.8573

The values of M_{sat}, D, S and P were obtained from related plots and calculated by using Eqs. (6), (7), (8), respectively

molecules diffusion in the poly(butylene succinate) (PBS)/Padauk sawdust composite.

Furthermore, the thermodynamic solubility (S) and permeability (P) variables were determined to further clarify the behavior of water absorption kinetics. The solubility was correlated to the absorption of the penetrant to an extent, which can be estimated by Eq. (7), as proposed by Jena et al. [45] as follows:

$$S = \frac{m_w}{m_c}, \tag{7}$$

where m_w and m_c represent the mass of water absorbed at saturation and the biocomposite samples mass, respectively. Also, the permeability coefficients were identified by determining the diffusion and absorption net product that is expressed by the following relation [45]:

$$P = D \times S. \tag{8}$$

From Table 4, it can be seen that both S and P variables increased with chitosan loading. The result obtained was correlated to the diffusion coefficient discussed before. Higher chitosan content reduced the filler–matrix interaction which enhanced chitosan dissolution into water molecules. This facilitated permeation of penetrant through the biocomposites, leading to the higher S and P values. A similar finding was reported by Chen et al. [46] in their studies of recycled polymer blend rice husk flour biocomposites.

Tensile properties of PLA/Cs biocomposites

Figure 6 demonstrates the influence of water absorption on tensile properties (tensile strength, tensile modulus, and elongation-at-break) of PLA-based biocomposites prepared with various chitosan loadings. It is observed in Fig. 6a, b that the dry sample with the incorporation of 2.5 php chitosan loading showed the highest tensile strength (54.6 ± 0.51 MPa) and tensile modulus (2.67 ± 0.01 GPa). This suggested that chitosan can be used as the reinforcement

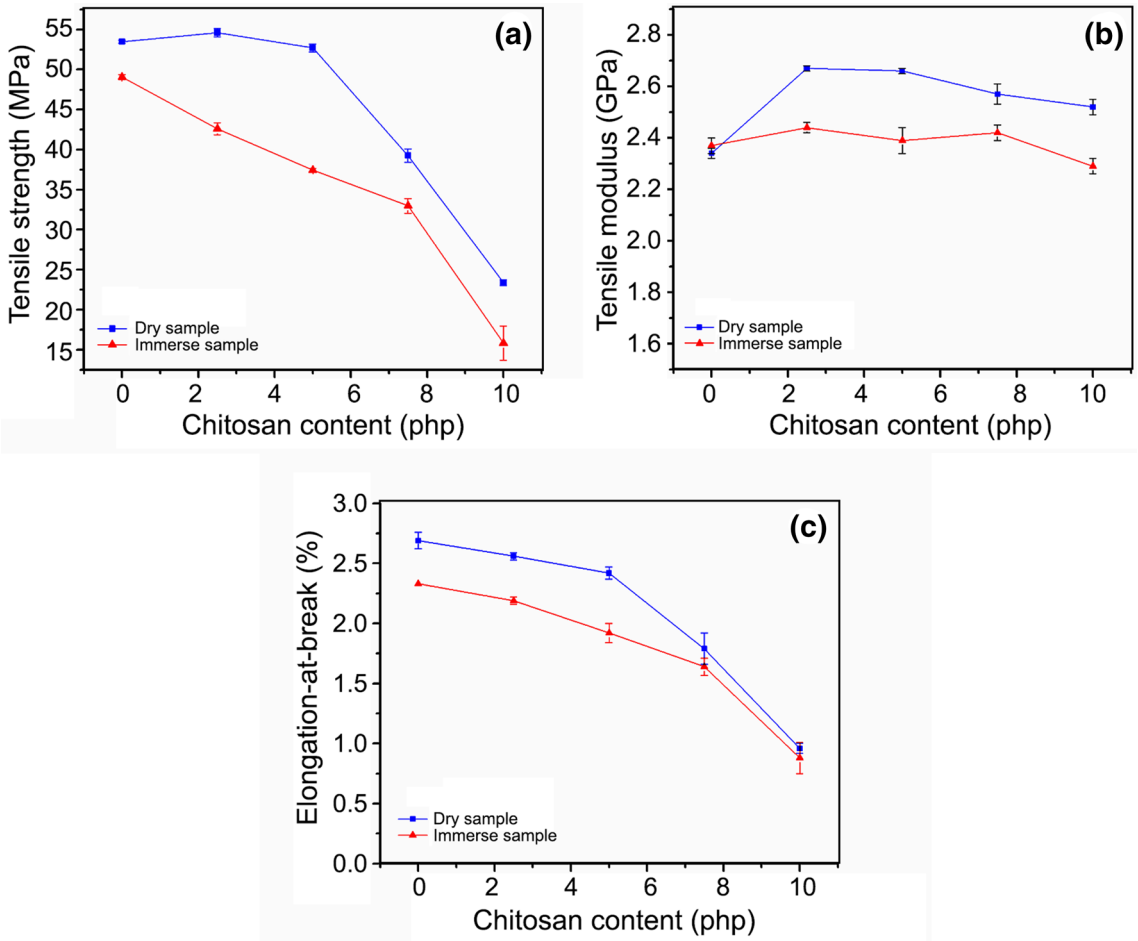

Fig. 6 Tensile properties of **a** tensile strength, **b** tensile modulus, and **c** elongation-at-break of dry and wet samples of PLA/Cs biocomposites as a function of chitosan loadings

filler in the PLA polymer matrix. However, further addition of chitosan content up to 10 php resulted in a gradual decrease in all tensile properties. This reduction occurred as a result of chitosan agglomeration in the PLA matrix, which reduced the interface bond strength, and thus lowered load transfers at the filler–matrix interface. This contributed to the deterioration of the biocomposite properties. The result was consistent with Bonilla et al. [13] who suggested that excess filler content could affect the resulting composites.

For the wet samples, it was demonstrated that PLA/Cs biocomposites exhibited lower tensile properties as compared to the dry samples. This may be affected by water molecules on the composite components which could alter the structure and behavior of the matrix-filler interface. As can be seen in Fig. 6a, the tensile strength of PLA/10Cs dropped drastically from 49 to 16 MPa with chitosan addition. This was attributed to the dissolution of the chitosan particulates because it leached into the water molecules, allowing greater water transport through the filler–matrix interface, and thus promoted a weak bonding at the interface region. This subsequently caused a failure in biocomposite, and thus reduced the tensile strength. The result was correlated to the study conducted by Priyanka and Palsule [47] who found the damage and cracks on the composites at high cellulose content in banana fiber-filled polypropylene composites.

A similar trend was observed in tensile modulus as it was reduced from 2.5 to 2.3 GPa at 10 php chitosan loading for dried and immersed samples, respectively. The presence of water molecules weakened the PLA/Cs interface by blocking their interaction, and thus lowered the stiffness of the hydrated biocomposite. This was consistent with the finding reported by Yu and Lau [48] for chitin-protein composite.

Meanwhile, reduction in elongation-at-break could be due to the separation of water-soluble components of the chitosan filler which worsened the filler–matrix adhesion; hence, lowered the biocomposite ability to elongate before rupture. A similar finding was described by Zahari et al. [49] in polypropylene/ijuk fiber composite.

Morphological characteristics of PLA/Cs biocomposites

Figure 7 represents the FESEM micrographs of the tensile fracture surface of pure PLA and PLA/Cs biocomposites before and after 50 days of water immersion at various chitosan loadings. The effects of chitosan loading and water absorption on filler–matrix adhesion were analyzed. For pure PLA, a smooth and homogeneous characteristic was observed on the fracture surface before and after the water absorption process as shown in Fig. 7a, b. This may be attributed to the hydrophobicity of PLA which absorbed less water, and thus an insignificant change was observed in the morphological characteristics of both wet and dry samples. In the case of PLA/Cs biocomposites, the dry specimens of less than 5 php chitosan loading exhibited relatively homogeneous filler dispersion; hence, they embedded well in the PLA matrix as presented in Fig. 7c, e. Besides, PLA/2.5Cs displayed the appearance of the tearing effect, which indicated a strong interaction on the matrix surface. This was in line with the tensile results which showed a slightly higher tensile property. Contrarily, PLA/10Cs of dry samples (Fig. 7g) demonstrated poor filler distribution due to chitosan agglomeration which implied the lowest tensile strength among the dry samples.

Nevertheless, the immersed biocomposite samples illustrated the rougher matrix surface with large cavities which signify polymer matrix degradation. The effect was obviously seen at higher chitosan loading of more than 5 php. This may be associated with the swelling effect induced during the immersion process. Swelling of the biocomposite initiated chitosan dissolution in an aqueous environment, and thus promoted hydrolytic degradation through the filler–matrix interface. This consequently contributed to filler detachment from the matrix surface as demonstrated by the filler pulled out phenomenon and cavities formation on the fractured surface, as shown in Fig. 7d, f of the wet samples. The results obtained were evidenced by deterioration in the tensile properties of the immersed samples discussed previously.

A similar observation was reported by Ghosh et al. [50] who found the presence of fiber pull-outs and micro-gaps in the fractured specimen of banana fiber reinforced-vinyl ester composites after water immersion, and thus contributed to the weak resin adhesion. Moreover, due to the chitosan hydrophilicity, the swelling capacity increased with the increase in chitosan loading; hence, stimulates faster water absorption. This explains the reason for the worst and rapid matrix degradation at 10 php of chitosan loading as observed in Fig. 7h.

Conclusion

The study on thermal behavior, water absorption kinetics, tensile and morphological properties of PLA/Cs biocomposites at various chitosan loadings was successfully conducted. It was noticed that the properties of PLA/Cs biocomposites were significantly influenced by the chitosan content. Through the thermal analysis study, the thermal stability of the biocomposites was reduced with the increased filler loading, but the degree of crystallinity of the neat PLA was enhanced significantly to an extent of 51%, which suggested that chitosan might act as a nucleating agent in the PLA/Cs biocomposites. The water absorption result showed that the maximum water uptake (M_{sat}) increased from 1.71 to 3.91% with chitosan addition of 2.5 php and 10 php, respectively,

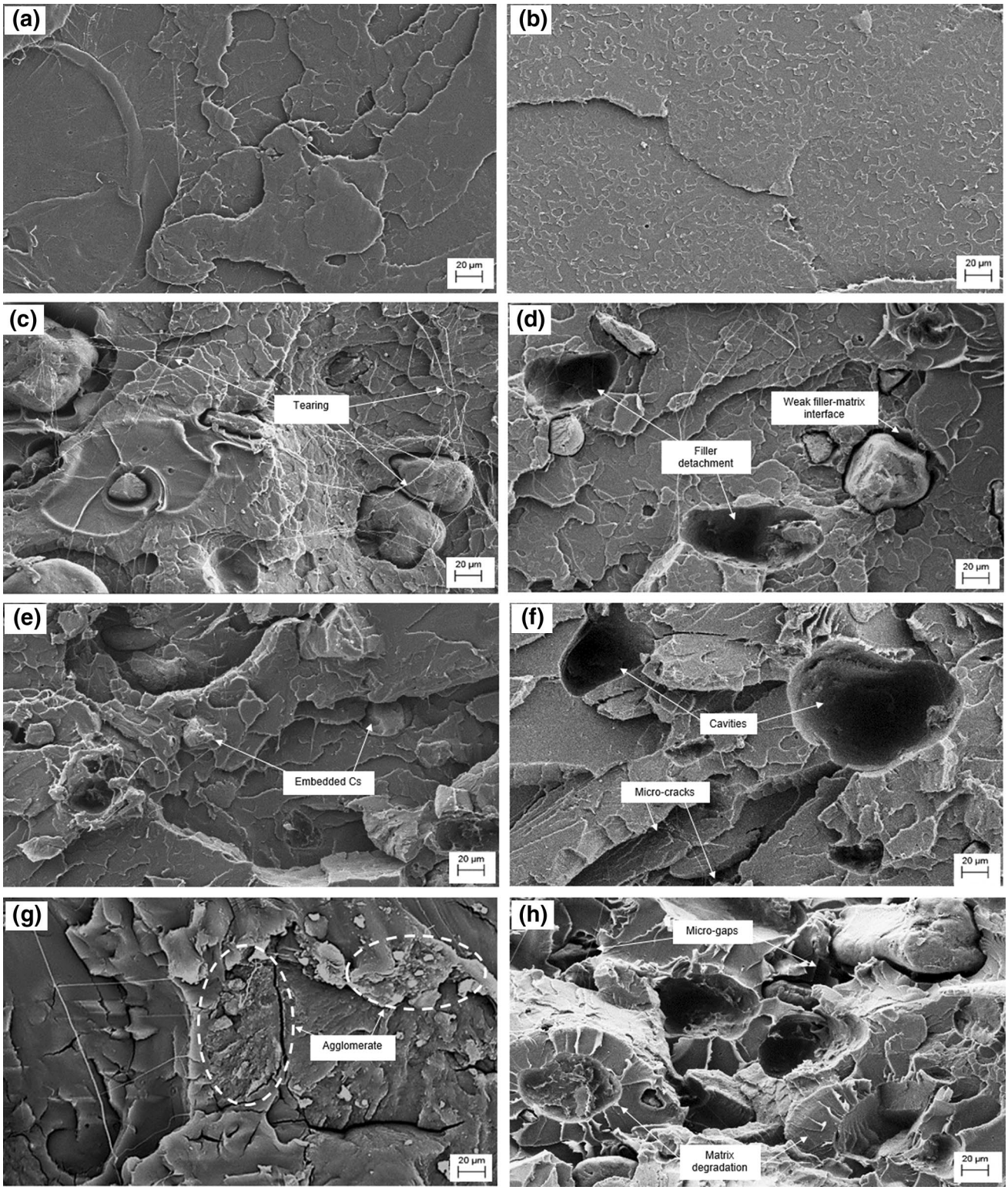

Fig. 7 FESEM micrographs of tensile fractured surfaces of PLA/Cs biocomposites before and after 50 days water immersion of **a**, **b** Pure PLA; **c**, **d** 2.5 php; **e**, **f** 5 php; **g**, **h** 10 php chitosan loadings, respectively under 300× magnification

which associated with a stronger water-filler interaction. The result obtained was correlated to the higher diffusion (D), solubility (S) and permeability (P) coefficients, which proposed acceleration in diffusion rate and water permeation through the PLA/Cs biocomposite. In addition, through the fitting curve of kinetics diffusion, the n values of less than 0.5 ($n < 0.5$) proposed that the water absorption of PLA/Cs biocomposites tended to approach the Fick's model. Meanwhile, the increase in k values confirmed the acceleration in water absorption as a shorter time was needed for the biocomposites to attain saturation. Tensile results of the dry samples at 2.5 php of chitosan loading showed increments in tensile strength and tensile modulus by 2% and 14%, respectively, relative to the neat PLA suggested an optimum filler content for the PLA/Cs biocomposites. However, water immersed specimens exhibited a slight reduction in tensile properties that diminished gradually with increased chitosan loading up to 10 php. This signified the hydrolytic polymer degradation as confirmed by FESEM analysis. The results of this study showed that PLA incorporated with higher chitosan loading promoted a slight deterioration in terms of thermal instability, tensile inability and matrix degradability of PLA/Cs biocomposites, especially upon the introduction of humid condition.

Acknowledgements The author would like to acknowledge the support from the Fundamental Research Grant Scheme (FRGS) under a Grant number of FRGS/1/2018/STG01/UNIMAP/03/3 from the Ministry of Education of Malaysia.

Author contributions All authors contributed to the study, main conceptual ideas and design. HI had supervised the project and NHIK conducted the experiment, collected and analyzed the data and wrote the manuscript with consultation and input from all authors. AR assisted in the thermal analysis study and SST helped to perform the water absorption kinetics. All authors have read and commented on the first draft of the manuscript and approved the submitted final version.

Funding This work was supported by the Ministry of Education of Malaysia under the Fundamental Research Grant Scheme (FRGS) (FRGS/1/2018/STG01/UNIMAP/03/3).

Compliance with ethical standards

Conflict of interest The authors declare that there is no conflict of interest.

References

1. Jambeck JR, Geyer R, Wilcox C, Siegler TR, Perryman M, Andrady A, Narayan R, Law KL (2015) Plastic waste inputs from land into the ocean. Science 347:768–771
2. New Straits Times (2020) Report: Malaysians Asia's biggest plastic consumers. https://www.nst.com.my/news/nation/2020/02/566374/report-malaysians-asias-biggest-plastic-consumers. Accessed 9 Mar 2020
3. Ramasamy S, Ismail H, Munusamy Y (2015) Soil burial, tensile properties, morphology, and biodegradability of (rice husk powder)-filled natural rubber latex foam. J Vinyl Addit Technol 21:128–133
4. Cao XV, Ismail H, Rashid AA, Takeichi T, Vo-Huu T (2014) Effect of filler surface treatment on the properties of recycled high-density polyethylene/(natural rubber)/(kenaf powder) biocomposites. J Vinyl Addit Technol 20:218–224
5. Han W, Ren J, Xuan H, Ge L (2018) Controllable degradation rates, antibacterial, free-standing and highly transparent films based on polylactic acid and chitosan. Colloid Surface A 541:128–136
6. Zaaba NF, Ismail H (2019a) A review on tensile and morphological properties of poly (lactic acid) (PLA)/thermoplastic starch (TPS) blends. Polym Plast Technol Mater 58:1945–1964. https://doi.org/10.1080/25740881.2019.1599941
7. Leu YY, Chow WS (2011) Kinetics of water absorption and thermal properties of poly(lactic acid)/organomontmorillonite/poly(ethylene glycol) nanocomposites. J Vinyl Addit Technol 17:40–47
8. Frone AN, Berlioz S, Chailan J-F, Panaitescu DM, Donescu D (2011) Cellulose fiber-reinforced polylactic acid. Polym Compos 32:976–985
9. Hassan A, Balakrishnan H, Akbari A (2013) In: Thomas S, Visakh PM, Mathew AP (eds) Advances in natural polymers: composites and nanocomposites. Springer, Berlin
10. Alias NF, Ismail H (2019) An overview of toughening polylactic acid by an elastomer. Polym Plast Technol Mater 58:1399–1422
11. Claro PIC, Neto ARS, Bibbo ACC, Mattoso LHC, Bastos MSR, Marconcini JM (2016) Biodegradable blends with potential use in packaging: a comparison of PLA/chitosan and PLA/cellulose acetate films. J Polym Environ 24:363–371
12. Zakaria Z, Islam MS, Hassan A, Mohamad Haafiz MK, Arjmandi R, Inuwa IM, Hasan M (2013) Mechanical properties and morphological characterization of PLA/chitosan/epoxidized natural rubber composites. Adv Mater Sci Eng. https://doi.org/10.1155/2013/629092
13. Bonilla J, Fortunati E, Vargas M, Chiralt A, Kenny JM (2013) Effects of chitosan on the physicochemical and antimicrobial properties of PLA films. J Food Eng 119:236–243
14. Ragunathan S, Mustaffa Z, Kamarudin H, Sam ST, Ismail H (2017) The effect of polypropylene maleic anhydride on polypropylene/(recycled acrylonitrile butadiene rubber)/(sugarcane bagasse) composite. J Vinyl Addit Technol 23:228–233
15. Zaaba NF, Ismail H (2019b) Effects of natural weathering on the degradation of alkaline-treated peanut shell filled recycled polypropylene composites. J Vinyl Addit Technol 25:26–34. https://doi.org/10.1002/vnl.21655
16. Ali F, Awale RJ, Mirghani MES, Anuar H, Samat N (2016) Preparation and characterization of plasticized polylactic acid/starch blend. J Teknol 78:7–12
17. Zaaba NF, Ismail H (2019c) The influence of different compounding sequence and peanut shell powder loading on properties of polylactic acid/thermoplastic corn starch biocomposites. J Vinyl Addit Technol. https://doi.org/10.1002/vnl.21756
18. Ismail H, Zaaba NF (2012) Tensile properties, degradation behavior, and water absorption of sago starch plastic films. J Vinyl Addit Technol 8:235–240
19. Das G, Biswas S (2016) Physical, mechanical and water absorption behaviour of coir fiber reinforced epoxy composites filled with Al_2O_3 particulates. IOP Conf Ser Mater Sci Eng 115:012012. https://doi.org/10.1088/1757-899X/115/1/012012
20. Râpă M, Mitelut AC, Tănase EE, Grosu E, Popescu P, Popa ME, Rosnes JT, Sivertsvik M, Darie-Niţă RN, Vasile C (2016) Influence of chitosan on mechanical, thermal, barrier and

antimicrobial properties of PLA-biocomposites for food packaging. Compos Part B Eng 102:112–121
21. Torres-Hernández YG, Ortega-Díaz GM, Téllez-Jurado L, Castrejón-Jiménez NS, Altamirano-Torres A, García-Pérez BE, Balmori-Ramírez H (2018) Biological compatibility of a polylactic acid composite reinforced with natural chitosan obtained from shrimp waste. Materials (Basel) 11:1465. https://doi.org/10.3390/ma11081465
22. Husseinsyah S, Amri F, Husin K, Ismail H (2011) Mechanical and thermal properties of chitosan-filled polypropylene composites: the effect of acrylic acid. J Vinyl Addit Technol 17:125–131
23. Correlo VM, Pinho ED, Pashkuleva I, Bhattacharya M, Neves NM, Reis RL (2007) Water absorption and degradation characteristics of chitosan-based polyesters and hydroxyapatite composites. Macromol Biosci 7:354–363
24. Ismail H, Abdullah AH, Abu Bakar A (2011) Influence of acetylation on the tensile properties, water absorption, and thermal stability of (high-density polyethylene)/(soya powder)/(kenaf core) composites. J Vinyl Addit Technol 17:132–137
25. Xu Q, Cui Y, Wang X, Xia Z, Han C, Wang J (2010) Moisture absorption properties of wood-fiber-reinforced recycled polypropylene matrix composites. J Vinyl Addit Technol 16:50–57
26. Chung T-J, Park J-W, Lee H-J, Kwon H-J, Kim H-J, Lee Y-K, Tze WTY (2018) The improvement of mechanical properties, thermal stability, and water absorption resistance of an eco-friendly PLA/kenaf biocomposite using acetylation. Appl Sci 8:376. https://doi.org/10.3390/app8030376
27. Aranda-García FJ, González-Núñez R, Jasso-Gastinel CF, Mendizábal E (2015) Water absorption and thermomechanical characterization of extruded starch/poly(lactic acid)/agave bagasse fiber bioplastic composites. Int J Polym Sci. https://doi.org/10.1155/2015/343294
28. Móczó J, Kun D, Fekete E (2018) Desiccant effect of starch in polylactic acid composites. eXPRESS Polym Lett 12:1014–1024
29. Dong Y, Marshall J, Haroosh HJ, Mohammadzadehmoghadam S, Liu D, Qi X, Lau K-T (2015) Polylactic acid (PLA)/halloysite nanotube (HNT) composite mats: influence of HNT content and modification. Compos Part A Appl Sci Manuf 76:28–36
30. Tham WL, Poh BT, Mohd Ishak ZA, Chow WS (2016) Transparent poly(lactic acid)/halloysite nanotube nanocomposites with improved oxygen barrier and antioxidant properties. J Therm Anal Calorim 126:1331–1337
31. Petchwattana N, Sanetuntikul J, Sriromreun P, Narupai B (2017) Wood plastic composites prepared from biodegradable poly(butylene succinate) and Burma padauk sawdust (*Pterocarpus macrocarpus*): water absorption kinetics and sunlight exposure investigations. J Bionic Eng 14:781–790
32. Pal AK, Katiyar V (2017) Melt processing of biodegradable poly(lactic acid)/functionalized chitosan nanocomposite films: mechanical modeling with improved oxygen barrier and thermal properties. J Polym Res. https://doi.org/10.1007/s10965-017-1305-5
33. Li H, Huneault MA (2007) Effect of nucleation and plasticization on the crystallization of poly(lactic acid). Polymer 48:6855–6866
34. Backes EH, Pires LN, Costa LC, Passador FR, Pessan LA (2019) Analysis of the degradation during melt processing of PLA/biosilicate® composites. J Compos Sci 3:52. https://doi.org/10.3390/jcs3020052
35. Tee YB, Talib RA, Abdan K, Chin NL, Basha RK, MdYunos KF (2013) Thermally grafting aminosilane onto kenaf-derived cellulose and its influence on the thermal properties of poly(lactic acid) composites. BioRes 8:4468–4483
36. Valapa R, Pugazhenthi G, Katiyar V (2014) Thermal degradation kinetics of sucrose palmitate reinforced poly(lactic acid) biocomposites. Int J Biol Macromol 65:275–283
37. Rodríguez-Núñez JR, Domínguez-López A, Domínguez-López C, Owen PQ, López-Cervantes J, Sánchez-Machado DI, Rodríguez Félix DE, Jatomea MP, Caballero VP, Santana TJM (2017) Evaluation of physicochemical and antifungal properties of polylactic acid–thermoplastic starch–chitosan biocomposites. Polym Plast Technol Eng 56:44–54
38. Md Zubir NH, Sam ST, Zulkepli NN, Omar MF (2018) The effect of rice straw particulate loading and polyethylene glycol as plasticizer on the properties of polylactic acid/polyhydroxybutyrate-valerate blends. Polym Bull 75:61–76
39. Muñoz E, García-Manrique J-A (2015) Water absorption behaviour and its effect on the mechanical properties of flax fibre reinforced bioepoxy composites. Int J Polym Sci. https://doi.org/10.1155/2015/390275
40. Cui Z, Beach ES, Anastas PT (2011) Modification of chitosan films with environmentally benign reagents for increased water resistance. Green Chem Lett Rev 4:35–40
41. Lukitowati F, Indrani DJ (2018) Water absorption of chitosan, collagen, and chitosan/collagen blend membranes exposed to gamma-ray irradiation. Iran J Pharm Sci 14:57–66
42. Hosseinihashemi SK, Arwinfar F, Najafi A, Nemli G, Ayrilmis N (2016) Long-term water absorption behavior of thermoplastic composites produced with thermally treated wood. Measurement 86:202–208
43. Adhikary KB, Pang S, Staiger MP (2008) Long-term moisture absorption and thickness swelling behaviour of recycled thermoplastics reinforced with *Pinus radiata* sawdust. Chem Eng J 142:190–198
44. Witono JR, Noordergraaf IW, Heeres HJ, Janssen LPBM (2014) Water absorption, retention and the swelling characteristics of cassava starch grafted with polyacrylic acid. Carbohydr Polym 103:325–332
45. Jena H, Pradhan AK, Pandit MK (2014) Studies on water absorption behavior of bamboo–epoxy composite filled with cenosphere. J Reinf Plast Compos 33:1059–1068
46. Chen RS, Ab Ghani MH, Salleh MN, Ahmad S, Tarawneh MA (2015) Mechanical, water absorption, and morphology of recycled polymer blend rice husk flour biocomposites. J Appl Polym Sci 132:41494. https://doi.org/10.1002/app.41494
47. Priyanka PS (2013) Banana fiber/chemically functionalized polypropylene composites with in-situ fiber/matrix interfacial adhesion by Palsule process. Compos Interface 20:309–329. https://doi.org/10.1080/15685543.2013.799012
48. Yu Z, Lau D (2015) Molecular dynamics study on stiffness and ductility in chitin–protein composite. J Mater Sci 50:7149–7157
49. Zahari WZW, Badri RNRL, Ardyananta H, Kurniawan D, Nor FM (2015) Mechanical properties and water absorption behavior of polypropylene/ijuk fiber composite by using silane treatment. Proc Manuf 2:573–578
50. Ghosh R, Ramakrishna A, Reena G, Ravindra A, Verma A (2014) Water absorption kinetics and mechanical properties of ultrasonic treated banana fiber reinforced-vinyl ester composites. Proc Mater Sci 5:311–315